

Received: 2018.08.16
Accepted: 2018.10.22
Published: 2018.11.13

Impact of Hyperbaric Oxygen on Tissue Healing around Dental Implants in Beagles

Authors' Contribution:
Study Design A
Data Collection B
Statistical Analysis C
Data Interpretation D
Manuscript Preparation E
Literature Search F
Funds Collection G

A 1 **Juan Liao***
B 2 **Meng-Jun Wu***
A 1 **Yan-Dong Mu**
C 3 **Peng Li**
B 1 **Jun Go**

1 Department of Stomatology, Sichuan Academy of Medical Sciences and Sichuan Provincial People's Hospital, Chengdu, Sichuan, P.R. China
2 Department of Anesthesiology, Chengdu Women' and Children's Central Hospital, Chengdu, Sichuan, P.R. China
3 Department of Anesthesiology, Sichuan Academy of Medical Sciences and Sichuan Provincial People's Hospital, Chengdu, Sichuan, P.R. China

* Juan Liao and Meng-Jun Wu contributed equally to this study and shared first authorship

Corresponding Author: Yan-Dong Mu, e-mail: 109497731@qq.com

Source of support: This study was supported by the Research Fund "Youth Scientific and Technological Creative Team" from the Sichuan Office of Technology (2016TD0008)

Background: The impact of hyperbaric oxygen (HBO) on the healing of soft tissues around dental implants was studied in a beagle model.





Material/Methods: Beagle dogs were randomized to receive implants, followed by postoperative HBO therapy or not (n=10 per group). On postoperative days 3, 7, and 14, tissue specimens were paraffin-embedded and analyzed by hematoxylin-eosin and Masson staining, as well as immunohistochemistry against CD31.

Results: Scores for inflammation pathology based on hematoxylin-eosin staining and mean optical density of collagen fibers were significantly different between the HBO and control groups on postoperative days 3 and 7 ($P<0.05$), but not on day 14. Mean optical density due to anti-CD31 staining was significantly higher in the HBO group on postoperative days 3, 7, and 14 ($P<0.05$).

Conclusions: These results suggest that HBO may promote early osteogenesis and soft tissue healing after implantation.

MeSH Keywords: **Dental Implantation • Hyperbaric Oxygenation • Soft Tissue Infections**

Full-text PDF: <https://www.medscimonit.com/abstract/index/idArt/912784>

 2715  4  7  20



Background

In the 1970s, Professor Branemark first proposed the osseointegration theory, thus establishing the biological basis of modern oral implantology. Researchers worldwide continue to explore methods for achieving osseointegration between dental implants and bone tissues in order to accelerate healing and increase implant success rates [1]. These efforts have focused on optimizing implant shape and surface treatment. Despite advances, early osseointegration failure remains a significant cause of implant failure.

Some studies have suggested that hyperbaric oxygen (HBO) can improve implant success rates, especially in patients who smoke or have diabetes [1]. HBO treatment involves inhalation of pure oxygen at pressures >0.1 MPa (1 ATA). In the 1980s, Beumer et al. [2] first applied HBO in stomatology to treat patients with dental osteoradionecrosis. Since then, HBO has been applied in many fields of stomatology [3–5], including therapy following dental implantation. HBO has been shown in clinical studies to prevent infection, relieve post-implantation swelling, and promote wound healing. However, some experts have highlighted the high cost of HBO and suggested that it does not significantly increase implant success rates [6]. Most studies of HBO after dental implantation are summaries of clinical experiences; we are unaware of basic research into the effects of HBO on early stages of tissue healing around implants.

The present study used a beagle model of tissue implantation to examine the effects of HBO on soft tissue healing around dental implants. Analyses combined morphology, imaging, histology, and immunohistochemistry in order to gain initial insights into whether and how HBO may promote osseointegration and soft tissue healing.

Material and Methods

Experimental animals

A total of 20 beagles, 12 months old and weighing 9 kg to 10 kg, were obtained from the Experimental Animal Institute of Sichuan People's Hospital and housed individually in cages. None of the animals had tooth defects, caries, or inflammation in the oral cavity. Animal handling and experiments were carried out in accordance with the United States National Institutes of Health Guide for Care and Use of Laboratory Animals.

Experimental reagents and equipment

Paraformaldehyde powder, 3% pentobarbital sodium, EDTA, chloroformaldehyde, dental implants, and implantation instruments were purchased from Straumann (Switzerland).

The animal HBO chamber was obtained from Hongyuan Oxygen Industrial (Yantai, China), the ImagePro Plus 6.0 image analysis was purchased from Media Cybernetics (USA), and an instrument for measuring impact stability quotient (ISQ) was from Osstell Medical Equipment (Gothenburg, Sweden). A BA200 digital trinocular microscope-camera imaging system was purchased from Motic China Group. Microtomes (type 2015, 1600 hard tissue) were obtained from Leica (Germany). A Kodak 2100 oral x-ray machine and Kodak 9000 cone beam computed tomography machine were purchased from Carestream Health.

Dental implantation

All dogs received general anesthesia of 3% pentobarbital sodium, and the local surgical area was injected with mepivacaine hydrochloride for infiltration anesthesia. A flap was created and mandibular third premolars were extracted bilaterally using a minimally invasive technique. A hole was prepared using standard methods in the distal socket of each edentulous area, in the direction of the long axis of the tooth. Dental implants (total of 64) were performed immediately, with a <2 mm separation between the implant and the surrounding bone walls. The upper edge of the rough surface of the implant was aligned with the alveolar ridge crest. The implant was covered with healing abutment (2 mm), and the wound was stitched. Animals were injected intramuscularly for 3 postoperative days with penicillin G sodium (800 000 U/d) to prevent infection.

Creation of oral soft tissue defects

The animals were randomly and evenly divided into HBO and control groups, and all underwent dental implantation. On postoperative day 1, HBO animals began the HBO treatment as described. The animal was sealed inside, and the pressure was increased during 15 minutes from atmospheric pressure to 2.4 ATA, where it was maintained for 60 minutes, and then the pressure was allowed to decrease during 15 minutes. To prevent sparking during the pressure session due to animal movement, animals were kept in a custom-made wooden box with air holes; all metal parts of the box were wrapped with gauze. Control dogs were not placed in the hyperbaric chamber and were instead maintained at atmospheric pressure throughout the 8-week period. Then, the portable implant machine was connected to a 5.0-mm tissue rotary drill, and circular soft tissue defect areas were created by removing mucoperiosteal flaps at the anterior, middle, and posterior hard palate. In addition, an undermining dissection was performed on the mucoperiosteal flap at the edge of the defect. Finally, a gelatin sponge was placed for hemostasis.

Sample analysis

On postoperative days 3, 7, and 14, tissues were collected from a randomly selected subset of dogs. Tissue was collected from the site of surgery and 2 mm around the site in the anterior, middle, and posterior palate. Tissues were trimmed, fixed in 4% paraformaldehyde for 72 hours, washed thoroughly in water, dehydrated in an alcohol gradient, cleared, immersed twice in paraffin, embedded in paraffin with an embedding machine, and sectioned into 3- μ m-thick slices using a microtome. Sections were stained using hematoxylin-eosin and Masson stain.

Histology

Decalcified, paraffin-embedded sections were prepared from left mandibles containing the implant. Non-decalcified hard tissue sections were prepared from right mandibles containing the implant. Decalcified paraffin sections were stained with hematoxylin-eosin and Masson trichrome stain, and examined with a BA200 digital trinocular microscopic camera system in order to compare the HBO and control groups in terms of inflammatory reactions and the formation and arrangement of new trabeculae. The BA200 digital trinocular microscopic camera system was used to observe sections stained with hematoxylin-eosin at magnifications of 40, 100, and 400x. The inflammatory cells were counted, and this number was used to determine grades of inflammation pathology based on previously described criteria (Table 1).

Mean optical density of collagen fibers

The BA200 system was also used to analyze Masson-stained sections. All tissues in each section were observed first under 100 \times magnification, then 3 fields were selected according to tissue size and expression for analysis at 400 \times magnification. Mean optical density in the images was measured using ImagePro Plus 6.0 (Media Cybernetics, USA).

CD31 immunohistochemistry

Tissue sections were mounted on slides, immersed in APES, then dried in an oven at 60°C for 60 minutes to cause tight adhesion. Sections were conventionally deparaffinized in water, treated with 30% H₂O₂-distilled water (1: 10, v/v) at room temperature for 10 minutes to inactivate endogenous peroxidases, and washed with distilled water 3 times. Antigen retrieval was performed by immersing sections in 0.01 M citric acid buffer (pH 6.0) and heating to boiling in a microwave oven, after which the oven was turned off. After waiting for 5 minutes, this step was repeated. Sections were left to cool, then washed twice with phosphate-buffered saline (PBS). Goat serum blocking solution was added dropwise onto sections, which were then

incubated at room temperature for 20 minutes. Sections were incubated with diluted primary rabbit anti-CD31 polyclonal antibody (1: 200) at 4°C overnight, washed 3 times with PBS (pH 7.2–7.4), incubated with secondary biotinylated goat anti-rabbit IgG at 37°C for 30 minutes, again washed 3 times with PBS (pH 7.2–7.4), incubated with horseradish peroxidase-labelled streptomycin ovalbumin reagent for 30 minutes at 37°C, and finally washed 4 times with PBS (pH 7.2–7.4). Antibody binding was visualized using DAB. Sections were then mildly counterstained using hematoxylin, then dehydrated, cleared, and mounted in neutral balsam.

The BA200 system was used to analyze CD31 immunohistochemistry. All tissues in each section were observed first at 100 \times magnification, then 3 fields were selected according to tissue size and expression for analysis at 400 \times magnification. Mean optical density of images was measured using ImagePro Plus 6.0.

Statistical analysis

Data were expressed as mean \pm SD and analyzed using SPSS 17.0. Pathology scores to assess levels of inflammatory cells were determined from sections stained with hematoxylin-eosin on postoperative days 3, 7, and 14 in the HBO group and the control group. Mean optical density of collagen fibers was determined in Masson-stained sections. Mean optical density of anti-CD31 staining was determined after appropriate immunohistochemistry. In all 3 analyses, inter-group differences were assessed using the LSD test when variance of data was homogeneous based on Levene's test, or using the corrected Welch method when variance was not homogeneous. Differences were assessed using one-way ANOVA. Statistical significance was defined as $P < 0.05$.

Results

Gross morphology of oral soft tissue defect healing

By postoperative day 3, oral sutures in all 20 dogs had dissolved. Mild inflammatory reaction was observed in the wounds of the HBO group, while the inflammatory reactions were more severe in the control group, and the wound edge showed redness and swelling. By postoperative day 7, the healed area covered two-thirds of the original wound area in the HBO group, the wound edge showed no obvious inflammation, and the center showed no obvious depression. In the control group, the healed wound area covered less than one half of the original wound area, the center showed obvious depression, and redness and swelling were still obvious. By postoperative day 14, the mucosal epithelium covering the wound surface was intact in the HBO group, there was no tissue depression, and there

Table 1. Scoring system for inflammation pathology in sections stained with haematoxylin-eosin.

Grade	Microscopy findings	Score
–	Basically normal, few or no inflammatory cells	0
+	Scattered infiltration of a small number of inflammatory cells	1
++	Between + and +++	2
+++	Extensive diffuse inflammatory cell infiltration; inflammatory granulomatous lesions caused by multinucleated giant cells can be observed	3

Adapted from ref. [7].

Table 2. Comparison of mean optical density of anti-CD31 staining at different times after surgery.

Group	Postoperative day		
	3	7	14
HBO	0.3235±0.0095*	0.3184±0.0018*	0.3502±0.0007*
Control	0.2624±0.0005	0.2780±0.0042	0.2790±0.0011

Values are mean ±SD (n=4). * P<0.05 vs. control group

Table 3. Grading of inflammation pathology in tissue sections at different times after surgery.

Group	Postoperative day		
	3	7	14
HBO	2.1250±0.3535*	1.3750±0.74402*	0.8750±0.35355
Control	2.8750±0.353	2.1250±0.35355	1.0±0.00

Values are mean ±SD (n=4). * P<0.05 vs. control group

was no scar formation. In the control group, the healed tissues on the wound surface still showed a depression, but the base had mucosal epithelium coverage.

Inflammation pathology was graded according to the criteria in Table 2, and differences between groups were assessed for significance as described in methods. Inflammation scores were significantly different between the HBO and control groups on postoperative days 3 and 7, but not day 14 (Table 3).

Histopathology and inflammation based on hematoxylin-eosin staining

On postoperative day 3, the HBO group showed absence of epidermis, subcutaneous tissue was necrotic, and staining was mostly red. Neutrophil infiltration was extensive, and lymphocytes were few. Fibrous connective tissue hyperplasia and residual gelatin sponge were observed (Figure 1A). Tissue from the control group showed massive subcutaneous tissue necrosis and red staining. Tissue structure was unclear and loose, and it showed edema and widening. Connective tissues

were dissolved, and subcutaneous blood vessels showed significant congestion and edema. Residual subcutaneous tissues presented a mesh structure. There was extensive neutrophil and eosinophil infiltration. Large necrotic areas and gelatin sponge residue were observed (Figure 1B).

At postoperative day 7, the HBO group showed active cell proliferation in fibrous connective tissues, new capillary hyperplasia, and a small amount of inflammatory cell infiltration. Formation of granulation tissue was better in the HBO group than in the control group, and there was no infection (Figure 2A). In the control group, fibrous connective tissue hyperplasia was obvious in the epidermis, few new capillaries were observed, and no infection was present, inflammatory cell infiltration was extensive, granulation tissue had formed, and the degree of granulation tissue repair was similar to that in the HBO group (Figure 2B).

At postoperative day 14, tissue from the HBO group showed new granulation tissues that had advanced to the surface to phagocytose, dissolve, digest, replace, and clear necrotic tissues. Many wounds were filled with connective tissue and repair of

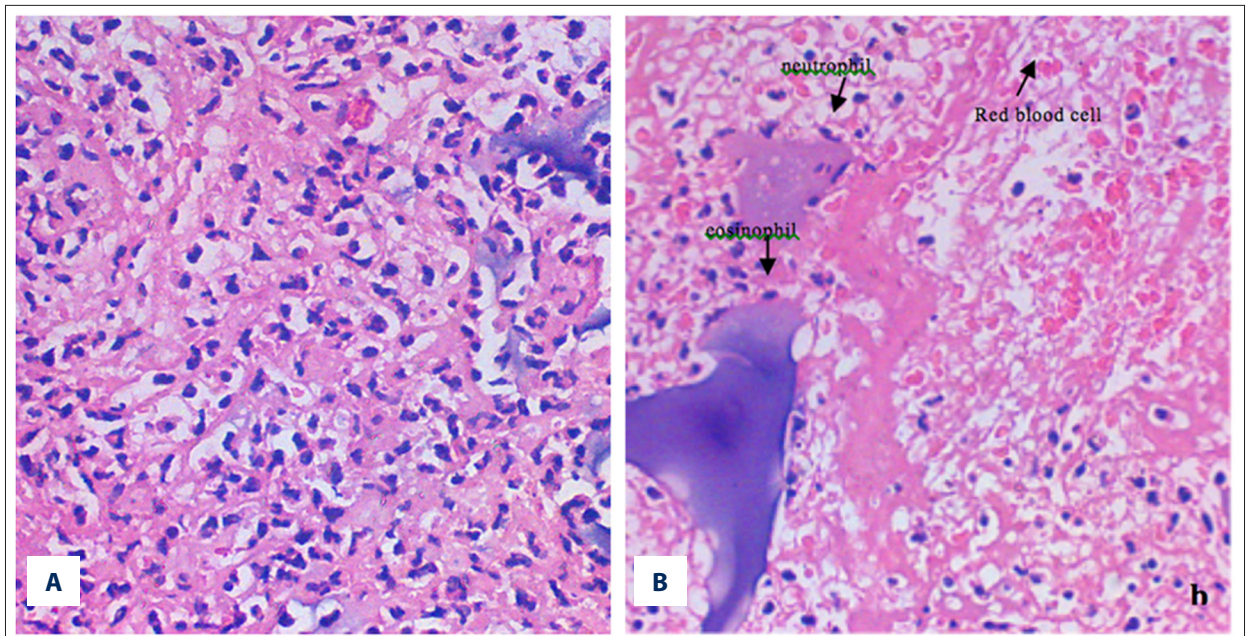


Figure 1. Images of tissue sections stained with hematoxylin-eosin from the HBO group (A) and control group (B) on postoperative day 3. Image at 400× magnification.

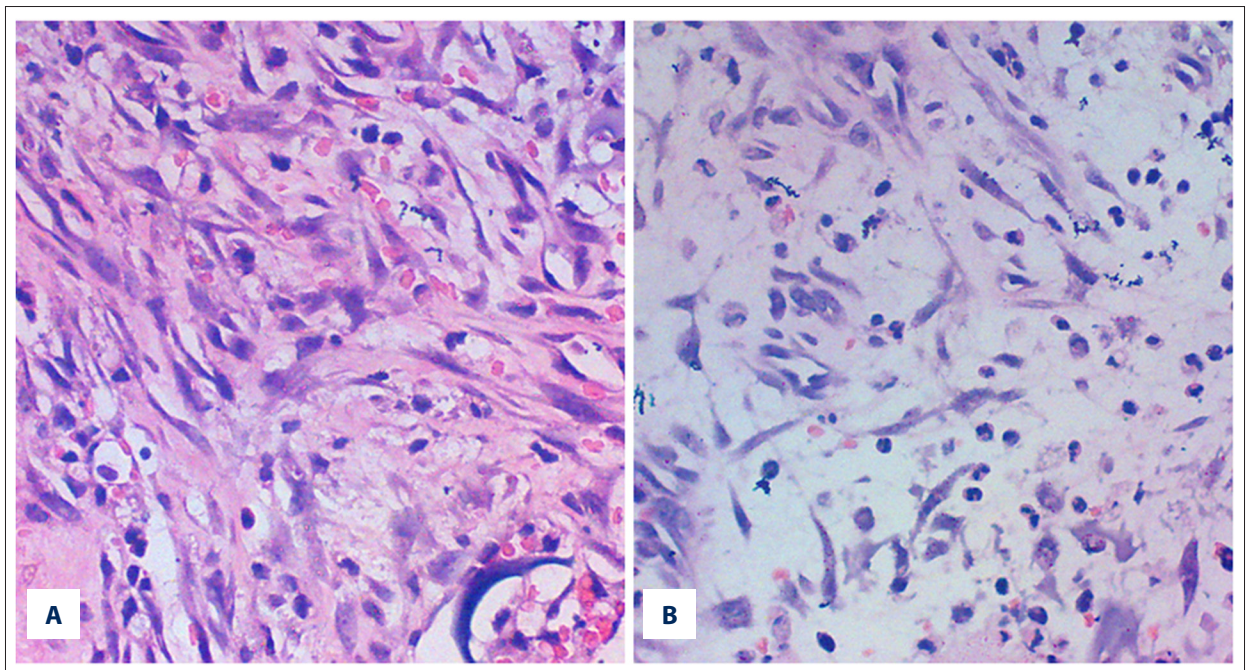


Figure 2. Images of tissue sections stained with hematoxylin-eosin from the HBO group (A) and control group (B) on postoperative day 7. Image at 400× magnification.

the wound surface was excellent. Only some inflammatory cell infiltration was observed (Figure 3A). Similar results were observed in the control group (Figure 3B).

Masson staining and mean optical density of collagen fibers

After Masson staining, collagen fibers in tissue sections appeared blue; red blood cells, orange; muscle fibers, cellulose, muscles, and cytoplasm, red; and nuclei, dark blue.

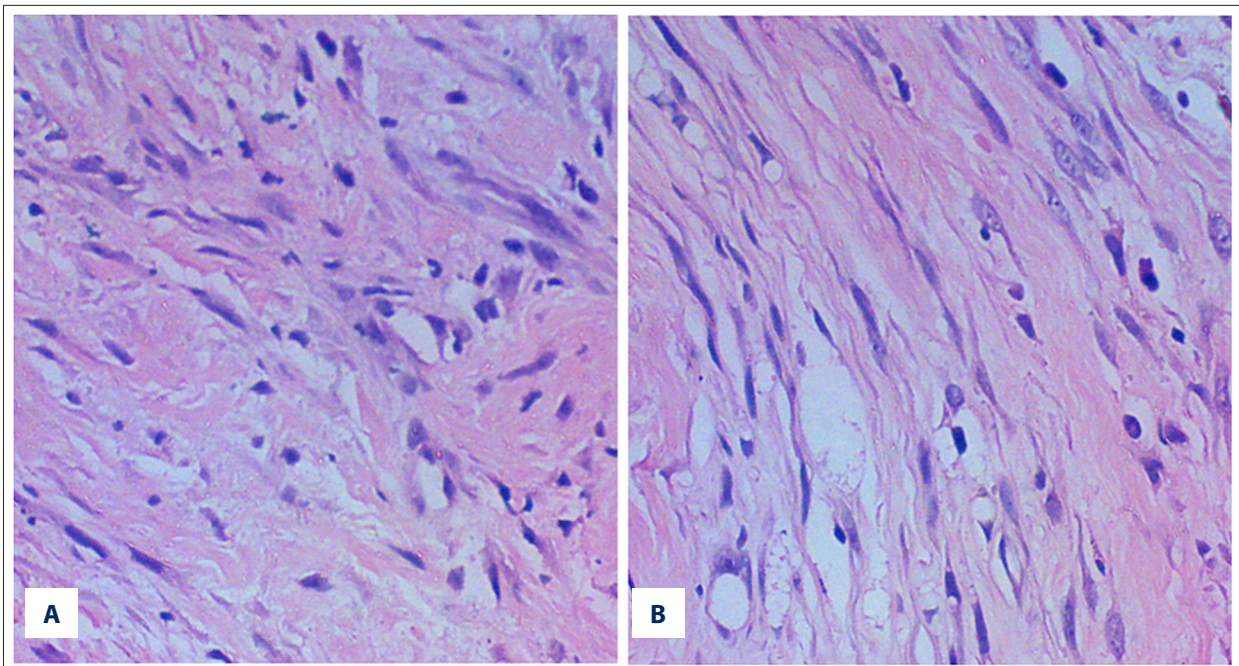


Figure 3. Images of tissue sections stained with hematoxylin-eosin from the HBO group (A) and control group (B) on postoperative day 14. Image at 400× magnification.

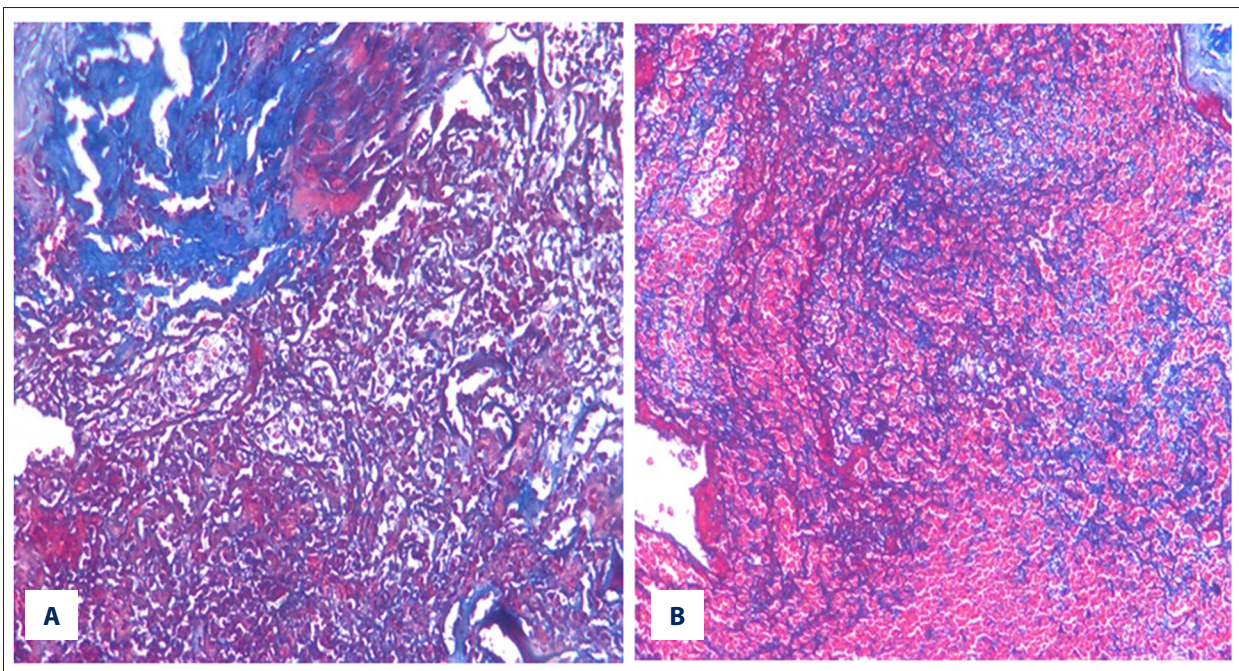


Figure 4. Images of tissue Masson-stained sections from the HBO group (A) and control group (B) on postoperative day 3. Image at 200× magnification. Blue fibrous tissue was surrounded by red blood cells in the HBO group. Massive red blood cells were observed in the control group. Surrounding blue fibrous tissue was less extensive than in the HBO group.

At postoperative day 3, the HBO group showed blue fibrous tissue formation and the presence of thin, disordered collagen fibers. Tissue from the control group showed massive red blood cells (Figure 4A, 4B). At postoperative day 7, the quantity of

collagen fibers increased in both groups, though they were more numerous and more ordered in the HBO group (Figure 5A, 5B). At postoperative day 14, collagen fibers in both groups showed an orderly arrangement (Figure 6A, 6B). Differences between

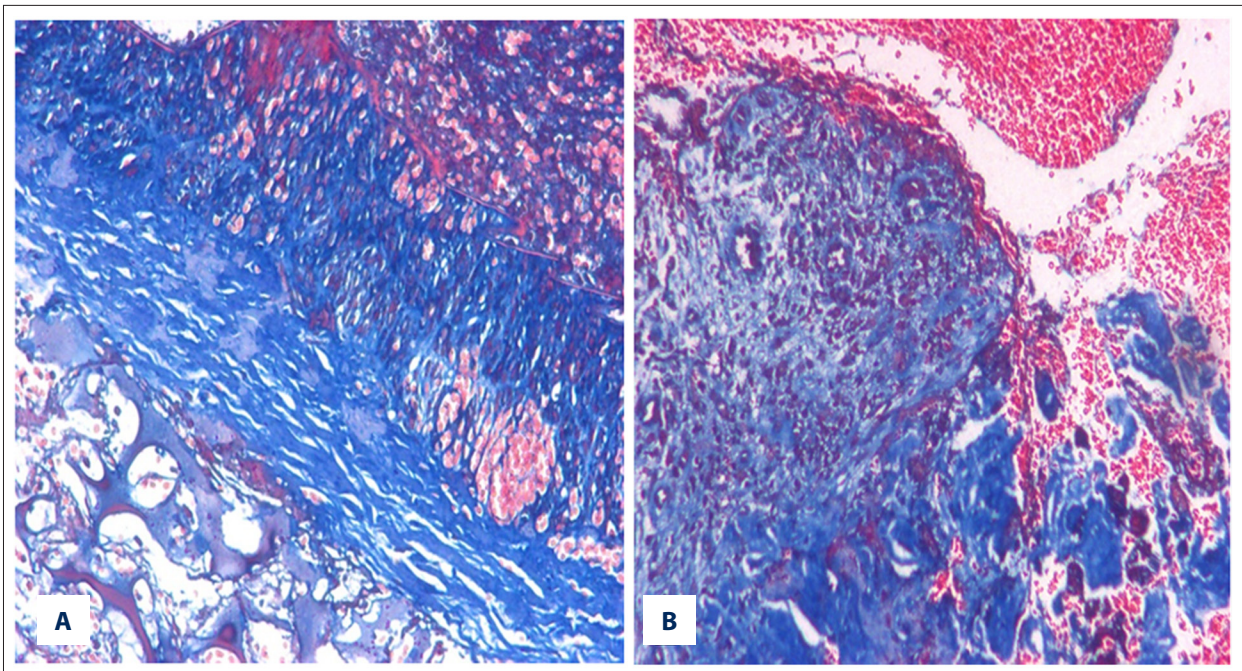


Figure 5. Images of tissue Masson-stained sections from the HBO group (A) and control group (B) on postoperative day 7. Image at 200× magnification. Collagen fibers were more abundant than at earlier time points in the control group, but still less abundant than in the HBO group.

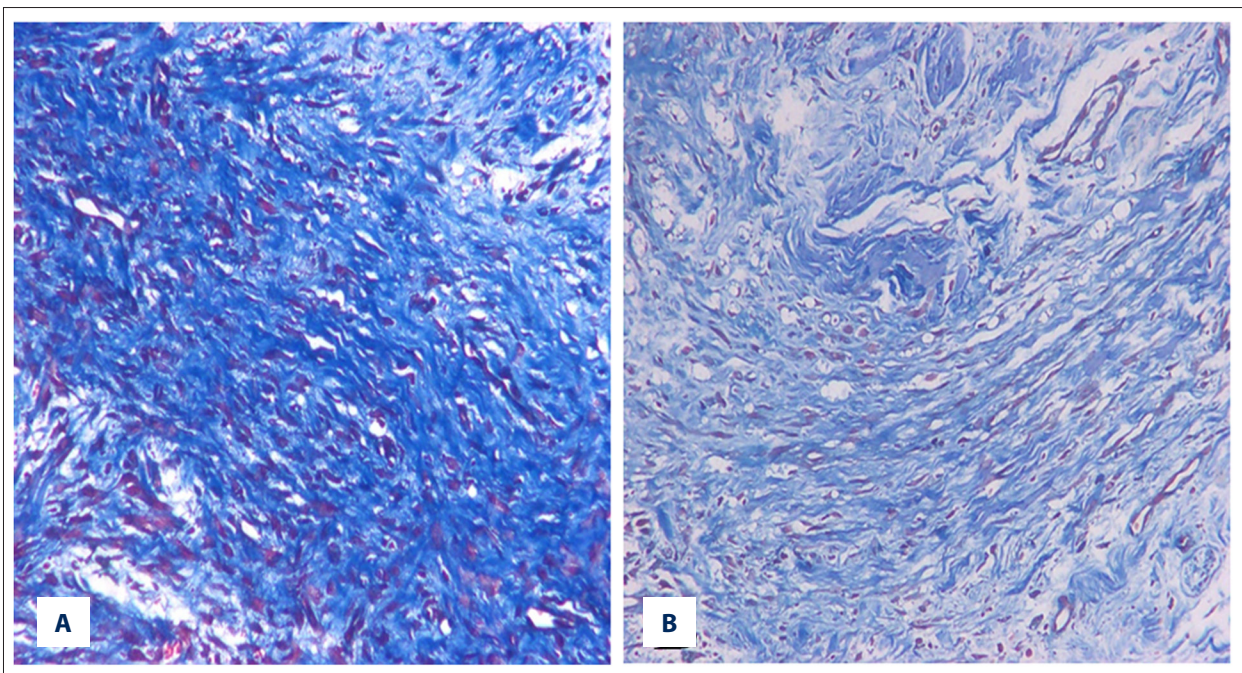


Figure 6. Images of tissue Masson-stained sections from the HBO group (A) and control group (B) on postoperative day 14. Image at 200× magnification.

groups in mean optical density of collagen fibers were assessed for significance. Mean optical density was significantly higher in the HBO group than the control group on postoperative days 3, 7, and 14 ($P < 0.05$; Table 4).

Anti-CD31 immunohistochemistry

In present immunostaining protocol, CD31 expression appeared light yellow or yellow-brown, lack of detectable CD31 appeared

Table 4. Comparison of mean optical density of collagen fibres at different times after surgery.

Group	Postoperative day		
	3	7	14
HBO	0.3700±0.0062*	0.4498±0.0032*	0.4409±0.0007
Blank	0.2780±0.0048	0.3817±0.0042	0.4350±0.0101

Values are mean ±SD (n=4). * P<0.05 vs. control group

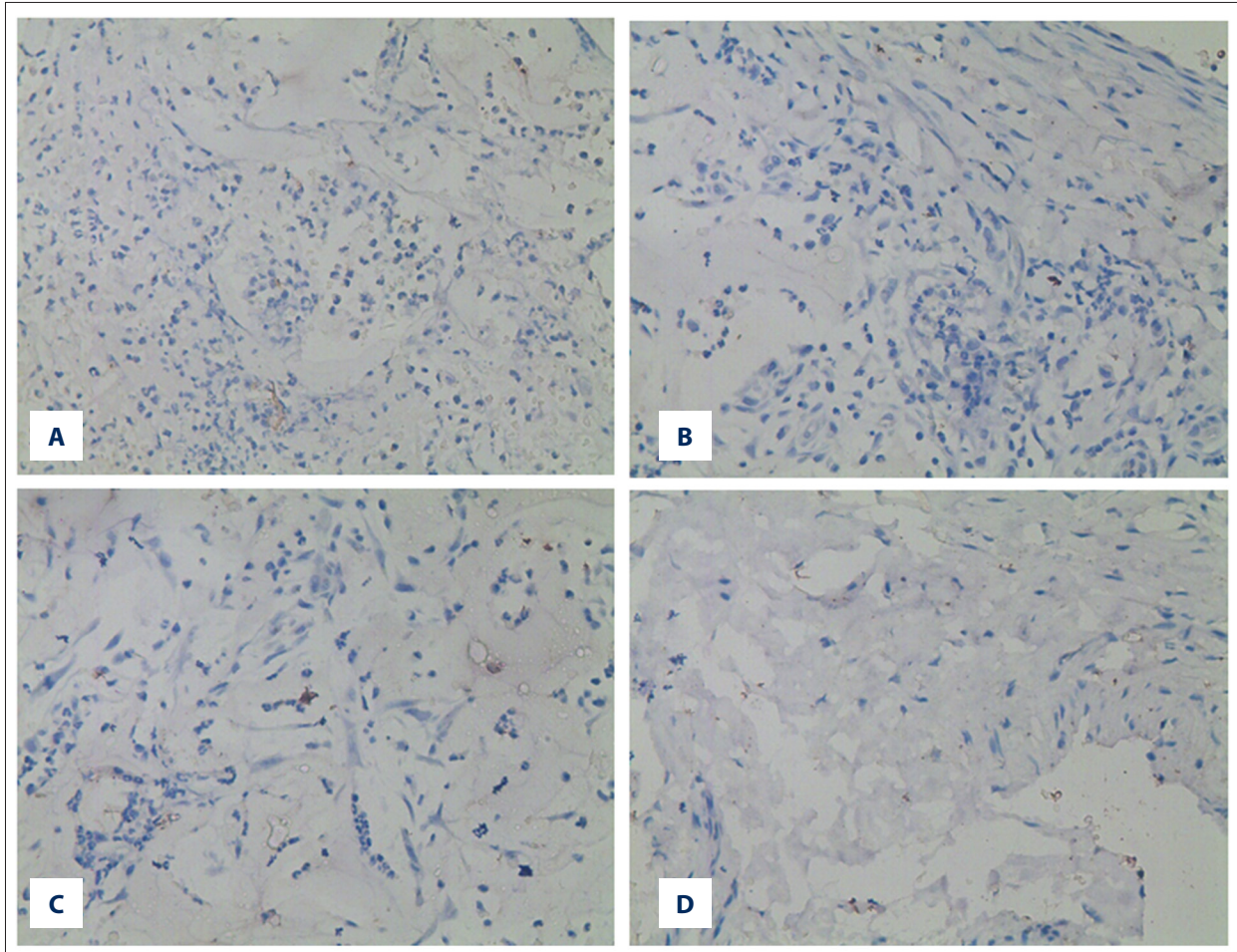


Figure 7. Anti-CD31 immunohistochemistry from the HBO group (A) and control group (B) on postoperative day 3, the HBO group (C) and control group (D) on postoperative day 7. Images were obtained at 400× magnification. Higher positive expression indicated greater formation of new capillaries in the control group.

blue, and the background appeared white. CD31 was expressed mainly in the cytoplasm and cell membrane, with more positive expression indicating greater formation of new capillaries at the wound surface (Figure 7).

Differences between groups in mean optical density of anti-CD31 staining were assessed for significance. Mean optical density was significantly higher in the HBO group than in the control group on postoperative days 3 and 7, but not day 14 (Table 2).

Discussion

The present study examined whether HBO, by improving the oxygen environment around implants, can influence the healing of soft tissue around implants. We found that, indeed, HBO promoted new soft tissue healing around implants in a beagle model. To our knowledge, this was this first preclinical study to demonstrate a relationship between HBO and soft tissue healing after implantation.

A beagle model is useful for analyzing the effects of HBO on soft tissue healing because collecting soft tissue from around implants in humans is challenging and usually does not provide enough material for histology. We therefore used the upper palate mucosa of beagles, which shows histomorphology similar to that of attached gingiva; this approach increased the sample collection area, simplified procedures, and increased reproducibility of experiments [7].

Hematoxylin-eosin staining of tissue sections showed that HBO effectively reduced inflammation and infection during wound healing, particularly during the first postoperative week. After acute surgical trauma, soft tissues immediately produce a locally ischemic, hypoxic environment. Inflammatory cells aggregate in the trauma area and synthesize inflammatory cytokines [8] and enzymes [9]. HBO may counteract these processes by rapidly increasing oxygen partial pressure in the blood, in turn enhancing oxygen metabolism and increasing ATP synthesis [10,11].

Consistent with a particularly strong effect of HBO on early stages of wound healing, we found that mean optical density of collagen fibers in Masson-stained sections was significantly higher in the HBO group than the control group on postoperative days 3 and 7, but not day 14. Collagen is the major component of extracellular matrix, and its synthesis and degradation directly affect the quality of wound surface repair [12]. It may be that in our experiments, HBO promoted collagen fiber synthesis relative to degradation early during wound repair, but this effect was cancelled out by increased fiber degradation during the subsequent remodeling phase of wound repair. Further studies should examine how HBO may promote collagen fiber formation in early stages of repair; previous work has suggested that HBO accelerates glycosaminoglycan synthesis and triggers hydroxylation during collagen release in fibroblasts [13].

In contrast to the stronger early-stage effects of HBO on inflammation and collagen fiber formation, HBO sustainably

promoted expression of the endothelial cell adhesion molecule CD31 through postoperative day 14, suggesting increased angiogenesis [14,15]. Angiogenesis begins immediately after wounding and provides the basis for healing and soft tissue repair and regeneration [16]. Some studies [17,18] have reported that HBO can increase angiogenesis during the early stage of burn recovery, and here we provide evidence that it can do the same for oral wounds. This angiogenic effect likely correlates with the observed stimulation of collagen fiber synthesis, which is required for capillary formation. Our results are consistent with the idea that HBO can promote wound epithelial formation and angiogenesis despite a reduction of macrophages [19,20].

There are some limitations in the present study. First, the animals in our study were otherwise healthy, whereas dental implantation in humans often co-occurs with other diseases. Second, it is different for metabolic and rheological properties between the beagle dental implantation and the complex human dental implantation.

Conclusions

Our study in a beagle model of dental implantation suggested that HBO can promote soft tissues reconstruction around implants, collagen tissue regeneration, and angiogenesis. These results, together with our previous work (in press) showing that HBO can reduce inflammatory reactions in bone, imply that HBO can function at all stages of soft tissue healing. Further study is needed to begin to identify the molecular mechanisms by which HBO promotes implant osseointegration. Such work should also explore the time course of HBO-mediated healing beyond the few points examined here, such as to determine optimal loading times under HBO.

Conflict of interest

None.

References:

1. Niezgodna JA, Serena TE, Carter MJ: Outcomes of radiation injuries using hyperbaric oxygen therapy: An observational cohort study. *Adv Skin Wound Care*, 2016; 29: 12–19
2. Beumer J, Harrison R, Sanders B, Kurrasch M: Osteoradionecrosis: Predisposing factors and outcomes of therapy. *Head Neck Surg*, 1984; 6: 819–27
3. Schoen PJ, Raghoebar GM, Bouma J et al: Rehabilitation of oral function in head and neck cancer patients after radiotherapy with implant-retained dentures: Effects of hyperbaric oxygen therapy. *Oral Oncol*, 2007; 43: 379–88
4. Oguz E, Ekinçi S, Eroglu M et al: Evaluation and comparison of the effects of hyperbaric oxygen and ozonized oxygen as adjuvant treatments in an experimental osteomyelitis model. *J Surg Res*, 2011; 171: e61–68
5. Nolen D, Cannady SB, Wax MK et al: Comparison of complications in free flap reconstruction for osteoradionecrosis in patients with or without hyperbaric oxygen therapy. *Head Neck*, 2014; 36: 1701–4
6. Esposito M, Grusovin MG, Patel S et al: Interventions for replacing missing teeth: Hyperbaric oxygen therapy for irradiated patients who require dental implants. *Cochrane Database Syst Rev*, 2008; 17: 123–34
7. Wang Z, Shi B, Lu D, Song Q: A histological study on healing process of palatal wound with denuded bone restored with transplanted buccal or palatal mucosa. *West China J Stomatol*, 2002; 20: 326–28
8. Yang F, Hu D, Bai X et al: Effects of vacuum sealing drainage on chemotaxis of inflammatory cells and secretion of inflammatory cytokines in skin wound of rabbits. *Chongqing Med*, 2012; 41: 686–88
9. Freedman JE, Vitseva O, Tanriverdi K: The role of the blood transcriptome in innate inflammation and stroke. *Ann NY Acad Sci*, 2012; 1207: 41–45

10. Ince B, Arslan A, Dadaci M et al: The effect of different application timings of hyperbaric oxygen treatment on nerve regeneration in rats. *Microsurgery*, 2016; 36: 586–92
11. Wang W, Jin L, Wang G: Effect of hyperbaric oxygen on survival rate of rats after resuscitation from traumatic shock. *Chin J Naut Med Hyperb Med*, 2008; 15: 19–24
12. Marx RE, Ames JR: The use of hyperbaric oxygen therapy in bony reconstruction of the irradiated and tissue-deficient patient. *J Oral Maxillofac Surg*, 1982; 40: 412–20
13. Kang TS, Gorti GK, Quan SY et al: Effect of hyperbaric oxygen on the growth factor profile of fibroblasts. *Arch Facial Plast Surg*, 2004; 6: 31–35
14. Valarmathi MT, Davis JM, Yost MJ et al: A three-dimensional model of vasculogenesis. *Biomaterials*, 2009; 30: 1098–112
15. Kasuya A, Tokura Y: Attempts to accelerate wound healing. *J Dermatol Sci*, 2014; 76: 169–72
16. Lancerotto L, Orgill DP: Mechanoregulation of angiogenesis in wound healing. *Adv Wound Care*, 2014; 3: 626–34
17. Bilic I, Petri NM, Bezic J et al: Effects of hyperbaric oxygen therapy on experimental burn wound healing in rats: A randomized controlled study. *Undersea Hyperb Med*, 2005; 32: 1–9
18. Sheikh AY, Rollins MD, Hopf HW, Hunt TK: Hyperoxia improves microvascular perfusion in a murine wound model. *Wound Repair Regen*, 2005; 13: 303–8
19. Lin S, Shyu KG, Lee CC et al: Hyperbaric oxygen selectively induces angiopoietin-2 in human umbilical vein endothelial cells. *Biochem Biophys Res Commun*, 2002; 296: 710–15
20. Sano H, Ichioka S, Sekiya N: Influence of oxygen on wound healing dynamics: Assessment in a novel wound mouse model under a variable oxygen environment. *PLoS One*, 2012; 7: e50212